

## Effects of (+)-tatarol, a diterpenoid antibacterial agent, on phospholipid model membranes

Vicente Micol <sup>a</sup>, C. Reyes Mateo <sup>a</sup>, Stuart Shapiro <sup>b</sup>, Francisco J. Aranda <sup>c</sup>,  
José Villalain <sup>a,\*</sup>

<sup>a</sup> Centro de Biología Molecular y Celular, Universidad 'Miguel Hernández', E-03202 Elche (Alicante), Spain

<sup>b</sup> Institut für orale Mikrobiologie, Universität Zürich, Plattenstrasse 11, Postfach, CH-8028 Zürich 7, Switzerland

<sup>c</sup> Departamento de Bioquímica y Biología Molecular, Universidad de Murcia, E-30080 Murcia, Spain

Received 17 October 2000; received in revised form 11 January 2001; accepted 18 January 2001

### Abstract

(+)-Tatarol, a highly hydrophobic diterpenoid isolated from *Podocarpus* spp., is inhibitory towards the growth of diverse bacterial species. (+)-Tatarol decreased the onset temperature of the gel to liquid-crystalline phase transition of DMPC and DMPG membranes and was immiscible with these lipids in the fluid phase at concentrations greater than 5 mol%. Different (+)-tatarol/phospholipid mixtures having different stoichiometries appear to coexist with the pure phospholipid in the fluid phase. At concentrations greater than 15 mol% (+)-tatarol completely suppressed the gel to liquid-crystalline phase transition in both DMPC and DMPG vesicles. Incorporation of increasing amounts of (+)-tatarol into DEPE vesicles induced the appearance of the H<sub>II</sub> hexagonal phase at low temperatures in accordance with NMR data. At (+)-tatarol concentrations between 5 and 35 mol% complex thermograms were observed, with new immiscible phases appearing at temperatures below the main transition of DEPE. Steady-state fluorescence anisotropy measurements showed that (+)-tatarol decreased and increased the structural order of the phospholipid bilayer below and above the main gel to liquid-crystalline phase transition of DMPC respectively. The changes that (+)-tatarol promotes in the physical properties of model membranes, compromising the functional integrity of the cell membrane, could explain its antibacterial effects. © 2001 Elsevier Science B.V. All rights reserved.

**Keywords:** Differential scanning calorimetry; Phospholipid vesicle; <sup>31</sup>P-Nuclear magnetic resonance; (+)-Tatarol; X-Ray diffraction; Fluorescence spectroscopy

Abbreviations:  $\langle r \rangle$ , steady-state fluorescence anisotropy;  $\Delta H$ , enthalpy change;  $\Delta\sigma$ , chemical shift anisotropy; DEPE, 1,2-di-elaidoyl-*sn*-glycero-3-phosphoethanolamine; DMPC, 1,2-dimyristoyl-*sn*-glycero-3-phosphocholine; DMPG, 1,2-dimyristoyl-*sn*-glycero-3-[phospho-*rac*-glycerol]; DSC, differential scanning calorimetry; <sup>31</sup>P-NMR, phosphorus nuclear magnetic resonance; PA-DPH, 3-(*p*-6-phenyl-1,3,5-hexatrienyl)phenylpropionic acid;  $T_c$ , onset temperature of the gel to liquid-crystalline phase transition

\* Corresponding author. Fax: +34-966-658-758;  
E-mail: boullon@umh.es

### 1. Introduction

Use of plants and plant products for medicinal purposes has roots tracing back to prehistoric times [1]. Amongst the classes of compounds that have proven to be of ethno-pharmacological importance are terpenoids, whose antimicrobial [2–8], antitumoral [9,10], anti-inflammatory [11] and cardiovascular [9,12] activities are the most representative biological activities described for these types of compounds.

During studies on the effects of phenolics towards oral microorganisms it has been observed that (+)-totarol (14-isopropyl-8,11,13-podocarpatrien-13-ol, see Fig. 1), a diterpenoid isolated from *Podocarpus* spp. and other plants, is an extremely potent inhibitor of supra- and subgingival bacteria [13]. (+)-Totarol, apart from being inhibitory towards the growth of diverse bacterial species [13–15], has also been shown to be effective against oxidative stress [16]. Other diterpenoids, particularly kauranes and secokauranes isolated from leaves of *Rabdosia trichocarpa*, also inhibit oral streptococci and the periodontopathogen *Porphyromonas gingivalis* [17]. Their mode(s) of action, as well as that of (+)-totarol, have not yet been described.

(+)-Totarol is a hydrocarbon containing a single phenolic moiety with an isopropyl group *ortho* to the hydroxyl group (Fig. 1). The minimal inhibitory concentration of (+)-totarol is some two orders of magnitude lower than that of thymol (unpublished results), a monoterpene commonly used as an oral antiseptic, with which (+)-totarol shares some structural features. While Haraguchi and co-workers [18] claimed that (+)-totarol functions at the level of energy-coupled bacterial respiration, (+)-totarol inhibited the growth of both facultative and obligate anaerobes cultured under strictly anaerobic conditions [13]. (+)-Totarol presents some similarities with thymol, although the hydrophobicity of (+)-totarol is much greater than that of thymol [19]. From the fact that thymol's principal mode of action is most likely through membrane rupture with ensuing leakage of intracellular constituents and collapse of transmembrane potentials [20] and from recent results of our group which show that (+)-totarol is embedded in the membrane [19], it seems reasonable to think that the mode of action of (+)-totarol might be at least partly attributable to its specific effect on membrane structure. Therefore, we have carried out a detailed study on the interaction of (+)-totarol with phospholipid model membranes composed of 1,2-dimyristoyl-*sn*-glycero-3-phosphocholine (DMPC), 1,2-dimyristoyl-*sn*-glycero-3-[phospho-*rac*-glycerol] (DMPG) and dielaidoyl-*sn*-glycero-3-phosphoethanolamine (DEPE) using differential scanning calorimetry (DSC), steady-state fluorescence anisotropy, small-angle X-ray diffraction and phosphorus nuclear magnetic resonance ( $^{31}\text{P}$ -NMR). The results ob-

tained in this work suggest that the potent antibacterial effects of (+)-totarol might be likely mediated by the formation of perturbed membrane structures.

## 2. Materials and methods

### 2.1. Chemicals

DMPC, DMPG and DEPE were obtained from Avanti Polar Lipids (Birmingham, AL, USA). Stock solutions were prepared in chloroform/methanol (2:1) and stored at  $-20^{\circ}\text{C}$ . (+)-Totarol was purchased from Industrial Research (Lower Hutt, New Zealand), and 3-(4-(6-phenyl)-1,3,5-hexatrienyl)phenylpropionic acid (PA-DPH) from Molecular Probes (Eugene, OR, USA). Water was twice-distilled in an all-glass apparatus and deionized using Milli-Q equipment (Millipore, Bedford, MA, USA). All other compounds were of analytical reagent grade.

### 2.2. Differential scanning calorimetry

Chloroform/methanol solutions containing 2.4  $\mu\text{mol}$  of total phospholipid (DMPC, DMPG or DEPE) and the appropriate amount of (+)-totarol were dried under a stream of oxygen-free  $\text{N}_2$  to obtain a thin film at the bottom of a small thick-walled glass tube, and the last traces of solvent were removed by keeping the samples under high vacuum for more than 3 h. Multilamellar vesicles were formed by incubating the dried lipid on 1.6 ml of buffer (10 mM HEPES, pH 7.4, 100 mM NaCl, 0.1 mM EDTA buffer) for 15 min at a temperature above the gel to liquid-crystalline transition (but below the temperature of the lamellar liquid-crystalline to hexagonal- $\text{H}_{\text{II}}$  transition for DEPE containing vesicles) with occasional and vigorous vortexing. Thermograms were recorded on a high-resolution Microcal MC-2 differential scanning microcalorimeter, equipped with a DA-2 digital interface and data acquisition utility for automatic data collection. Differences in the heat capacity between the sample and the reference cell, which contained only buffer, were obtained by raising the temperature at a constant rate of  $1^{\circ}\text{C}/\text{min}$  over the range from  $8^{\circ}\text{C}$  to  $45^{\circ}\text{C}$  for samples containing DMPC or DMPG, or from  $15^{\circ}\text{C}$  to  $75^{\circ}\text{C}$  for samples containing DEPE. A series

of three consecutive scans of the same sample were performed to ensure scan-to-scan reproducibility. Unless otherwise stated, the third scan was used for transition and enthalpy calculations. After the thermal measurements the phospholipid content of the sample volume was determined [21]. Partial phase diagrams for the phospholipid components were constructed as previously described [22]. The onset and completion temperatures of the transition peaks obtained from heating scans defined the solidus and fluidus lines of the diagrams.

### 2.3. $^{31}\text{P}$ -Nuclear magnetic resonance spectroscopy

For NMR analysis, 30  $\mu\text{mol}$  of the phospholipid and the appropriate amount of (+)-tatarol were mixed in chloroform and evaporated to dryness under a stream of oxygen-free  $\text{N}_2$ . The remaining traces of solvent were removed by storage for 5 h under high vacuum. HEPES buffer (0.3 ml) was added to the dry lipid mixtures and the samples were heated at a temperature above the transition temperature for 30 min with occasional and vigorous vortexing. The suspensions were transferred into conventional 5 mm NMR tubes and  $^{31}\text{P}$ -NMR spectra were obtained in the Fourier transform mode at different temperatures in a Varian Unity 300 spectrometer. All chemical shift values were quoted in parts per million (ppm) with reference to pure lysophosphatidylcholine micelles (0 ppm), positive values referring to low-field shifts. All spectra were obtained in the presence of a gated-broad band proton decoupling (10 W input power during acquisition time) and accumulated free induction decays were obtained from up to 2000 scans. A spectral width of 25 000 Hz, a memory of 32K data points, a 2 s interpulse time and an  $80^\circ$  radio frequency pulse were used. Prior to Fourier transformation, an exponential multiplication was applied resulting in a 100 Hz line broadening. The residual chemical shift anisotropy,  $\Delta\sigma$ , was calculated as 3 times the chemical shift difference between the high-field peak and the position of isotropically moving lipid molecules at 0 ppm [22].

### 2.4. Fluorescence spectroscopy

DMPC vesicles containing different (+)-tatarol concentrations were prepared as described for DSC

measurements. Aliquots of PA-DPH in *N,N'*-dimethylformamide ( $2 \times 10^{-4}$  M) were directly added to the lipid dispersion to obtain a probe/lipid molar ratio of 1:500. Samples were incubated well above the gel to liquid-crystalline phase transition temperature for 10 min and measurements were carried out immediately thereafter. Steady-state fluorescence anisotropy,  $\langle r \rangle$ , of PA-DPH was measured at different temperatures using an SLM-8000C spectrofluorimeter fitted with Glan-Thompson polarizers. The vertical and horizontally polarized emission intensities, elicited by vertically polarized excitation, were corrected for background scattering by subtracting the corresponding polarized intensities of a blank containing the unlabelled preparation. The *G*-factor, which accounts for the differential polarization sensitivity, was determined by measuring the polarized components of fluorescence of the probe with horizontally polarized excitation. Samples were excited at 350 nm (slit width, 1 nm) and fluorescence emission was recorded at 450 nm (slit width, 4 nm).

### 2.5. Small-angle X-ray diffraction

Samples for X-ray diffraction analysis were prepared essentially as described for DSC. Usually 10–15 mg of lipid were dried and resuspended in 1 ml of HEPES buffer, pelleted down in a bench microfuge and placed in the X-ray diffractometer sample holder. Nickel-filtered  $\text{Cu K}\alpha$  X-rays ( $\lambda = 1.54$  Å) were produced using a Philips generator (PW1830). X-Rays were focussed using a flat gold-plated mirror. Lipid dispersions were irradiated in aluminium holders with Mylar windows and diffractograms recorded using a linear position-sensitive detector (model 210, Bio-Logic, Grenoble, France). The sample temperature was kept within  $\pm 0.5^\circ\text{C}$ , using a circulating water bath, and the system was allowed to equilibrate for about 5 min at each temperature before measurements. The X-ray exposure times were typically 10–15 min for each sample. Calibration of the detector was carried out using crystalline cholesterol (d-spacing = 33.6 Å).

## 3. Results

The effect of (+)-tatarol on the thermotropic be-

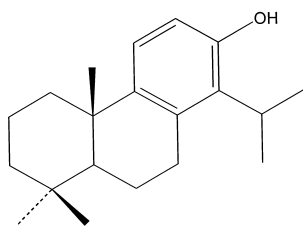


Fig. 1. Chemical structure of (+)-tatarol (14-isopropyl-8,11,13-podocarpatrien-13-ol).

behaviour of either DMPC or DMPG vesicles has been studied by DSC as shown in Fig. 2A and B, respectively. Addition of a low concentration (0.5 mol%) of (+)-tatarol drastically broadened the pretransition and slightly broadened the main gel to liquid-crystalline transition signal of DMPC (Fig. 2A). At (+)-tatarol concentrations equal or greater than 2 mol% there is a complete disappearance of the pretransition signal and a shift of the main transition signal of DMPC towards lower temperatures. Within the range 5–15 mol% (+)-tatarol complex patterns were observed, with a progressively downward  $T_c$  shift,

and the appearance of broad new peaks located near to the gel to liquid-crystalline phase transition signal of DMPC. At 10 mol% (+)-tatarol the transition has a broad, complex shape with a maximum at 21°C, although a shoulder discerned at higher temperatures indicates the presence of at least two different phospholipid populations. A very broad profile was observed at 15 mol% (+)-tatarol, and the main phase transition was completely abolished at 30 mol% (+)-tatarol.

A similar behaviour was observed for DMPG vesicles in the presence of increasing amounts of (+)-tatarol (Fig. 2B). The pretransition was abolished at very low concentrations of (+)-tatarol and the main transition shifted to lower temperatures upon increasing its concentration. On going from 2 to 15 mol% (+)-tatarol the transition progressively broadened but did not show the complex patterns observed in the DMPC samples. As it was found for DMPC, the main phase transition of DMPG was completely abolished at a concentration of 30 mol% (+)-tatarol.

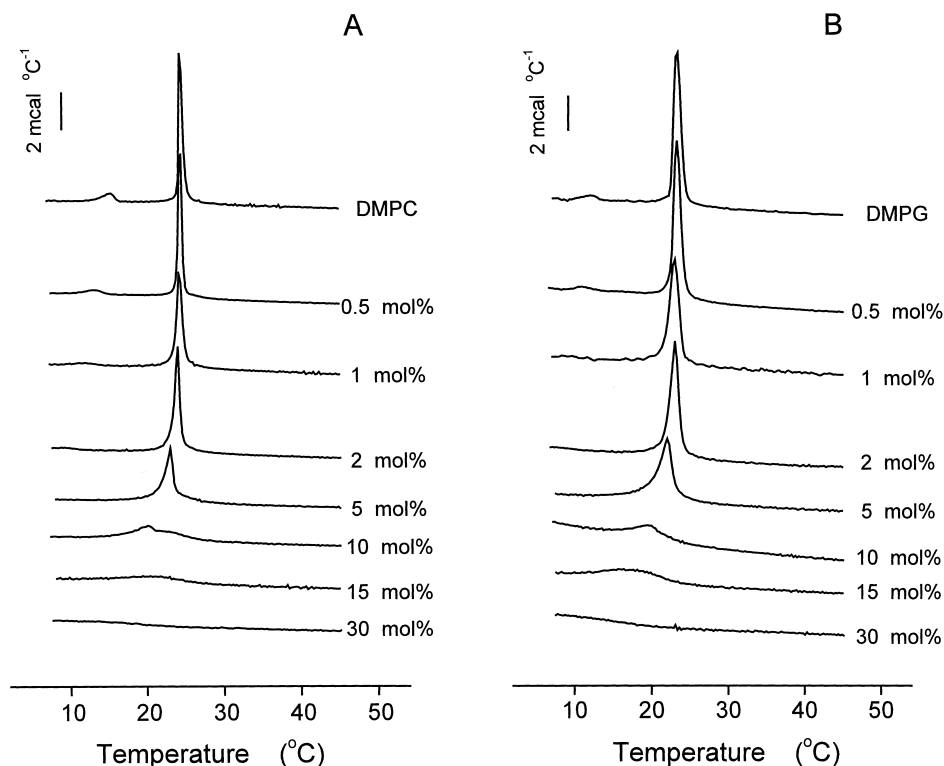


Fig. 2. Differential scanning calorimetry heating-scan thermograms for mixtures of (+)-tatarol plus (A) DMPC and (B) DMPG. Each sample contained the appropriate amount of (+)-tatarol (molar % of total) as indicated on the curves.

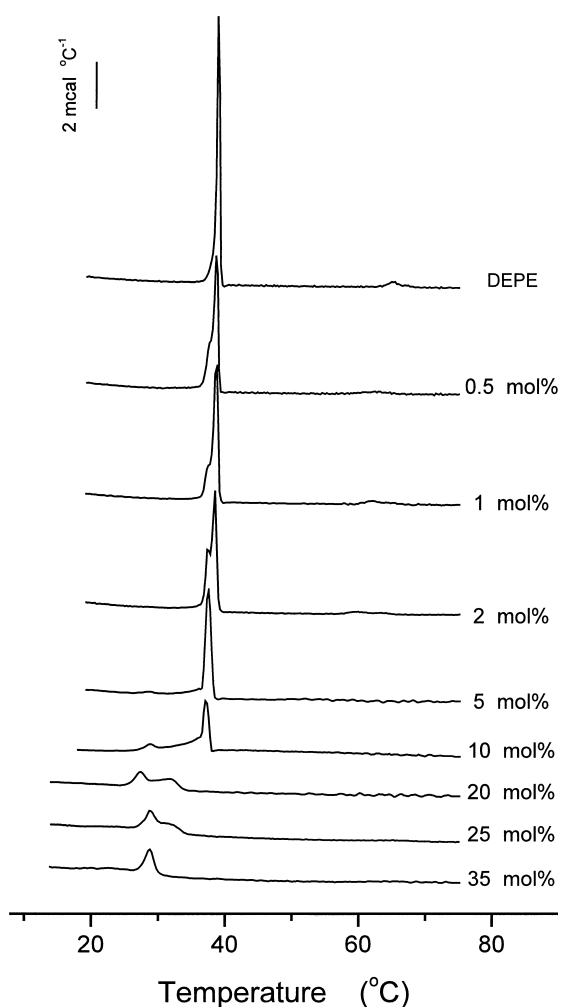


Fig. 3. Differential scanning calorimetry heating-scan thermograms for mixtures of (+)-tatarol plus DEPE. Each sample contained the appropriate amount of (+)-tatarol (molar % of total) as indicated on the curves.

We have studied the presence of (+)-tatarol-induced membrane perturbations on model membranes composed of DEPE by DSC (Fig. 3). Aqueous dispersions of DEPE can undergo a gel to liquid-crystalline ( $L_\beta \rightarrow L_\alpha$ ) phase transition in the lamellar phase (approx. 37°C) and, in addition, a lamellar liquid-crystalline to hexagonal- $H_{II}$  ( $L_\alpha \rightarrow H_{II}$ ) transition (approx. 65°C) [23]. In the presence of concentrations of (+)-tatarol as low as 0.5 mol%, a new transition occurs at the low-temperature side of the main gel-to-liquid phase transition (around 34°C) (Fig. 3). This new peak increased in area at the expense of the main peak when the amount of (+)-tatarol was increased, and became the predominant

peak at a concentration of 5 mol% (+)-tatarol. At 5 mol% another small peak was apparent at approx. 24°C. At (+)-tatarol concentrations between 5 and 35 mol% complex thermograms were observed, with new phases appearing at temperatures below the main phase transition temperature of the phospholipid. At 20 mol% (+)-tatarol the sharp peak found at 34°C was no longer observed and a broad transition coexisted with the 24°C peak. At 35 mol% (+)-tatarol only one transition was observed (Fig. 3). Incorporation of increasing amounts of (+)-tatarol into DEPE vesicles stabilized the  $H_{II}$  hexagonal phase: the  $L_\alpha \rightarrow H_{II}$  phase transition gradually decreased from 0.5 to 2 mol% (+)-tatarol and was no longer apparent above 2 mol% (+)-tatarol (Fig. 3).

The effects of (+)-tatarol on the transition enthalpies ( $\Delta H$ ) of the main gel to liquid-crystalline phase transitions of DMPC, DMPG and DEPE were also determined (Table 1). For DMPC and DMPG, the  $\Delta H$  decreased as a function of increasing concentrations of (+)-tatarol until a concentration of 30 mol% (+)-tatarol was reached, when the transitions disappeared. This decrease in  $\Delta H$  was nearly linear, despite the fact that several peaks with different widths were found in the thermograms at different phospholipid/(+)-tatarol molar ratios. A decrease in  $\Delta H$  was also found for DEPE as a function of increasing concentrations of (+)-tatarol, but it was not as significant as that found for DMPC and DMPG. We have calculated the average number of phospholipid molecules per molecule of (+)-tatarol as described previously [24], obtaining values of  $4.2 \pm 0.3$ ,  $4.6 \pm 0.23$  and  $1.9 \pm 0.26$  for DMPC, DMPG and DEPE respectively.

To discern how (+)-tatarol could affect the phase behaviour of DMPC and DEPE we have carried out  $^{31}\text{P}$ -NMR measurements at different temperatures.  $^{31}\text{P}$ -NMR is sensitive to local motion and orientation of the phosphate group in membrane phospholipids, and the macroscopic environment of the whole molecule determines the line shape of the  $^{31}\text{P}$ -NMR spectrum [25]. This phase sensitivity makes  $^{31}\text{P}$ -NMR a very suitable tool to follow the structural changes in biological and model membranes. DMPC and DEPE, when organized in bilayer structures, give rise to an asymmetrical  $^{31}\text{P}$ -NMR line shape with a high-field peak and a low-field shoulder, presenting a residual chemical shift anisotropy,  $\Delta\sigma$ , of around 36–

Table 1

Enthalpy changes ( $\Delta H$ , kcal/mol) for mixtures containing (+)-tatarol and DMPC, DMPG and DEPE at different (+)-tatarol mol fractions

Tatarol mol fraction	$\Delta H$ (kcal/mol)		Tatarol mol fraction	$\Delta H$ (kcal/mol)
	DMPC	DMPG		DEPE
0	5.9	6.9	0	8.3
0.005	5.6	6.6	0.005	7.4
0.01	5.0	6.3	0.01	7.0
0.02	4.9	6.1	0.02	6.5
0.05	4.2	5.5	0.05	7.4
0.10	4.0	3.3	0.1	6.15
0.15	2.0	2.5	0.2	5.45
			0.25	6.2
			0.35	5.9

40 ppm in the gel state and approx. 27–30 ppm in the liquid-crystalline state. In the  $H_{II}$  phase, due to rapid lateral diffusion of the phospholipid around the tubes of which this phase is composed, the chemical shift anisotropy is further averaged resulting in a line shape with reverse symmetry, i.e., a high-field shoulder and a low-field peak, with a 2-fold reduction in the absolute value of  $\Delta\sigma$  [22]. Incorporation of (+)-tatarol in DMPC membranes did not induce any significant change in the line shape of the  $^{31}\text{P}$ -NMR spectra when compared to the pure phospholipid (not shown for brevity). However, DEPE membranes containing as low as 2 mol% of (+)-tatarol showed a signal corresponding to the hexago-

nal- $H_{II}$  phase superimposed to a bilayer signal at temperatures much lower than that of the pure phospholipid (Fig. 4). At a concentration of 10 mol% of (+)-tatarol, a signal corresponding to the hexagonal- $H_{II}$  phase was observed at temperatures as low as 22°C.

The effect of the incorporation of (+)-tatarol on the phase adopted by the phospholipid membranes at different temperatures has also been studied by small-angle X-ray diffraction. In the case of DMPC model membranes and mixtures containing (+)-tatarol (not shown), the first and second order reflections appeared at a ratio of the lattice parameter of 1:1/2, indicating that the systems were always in the lamel-

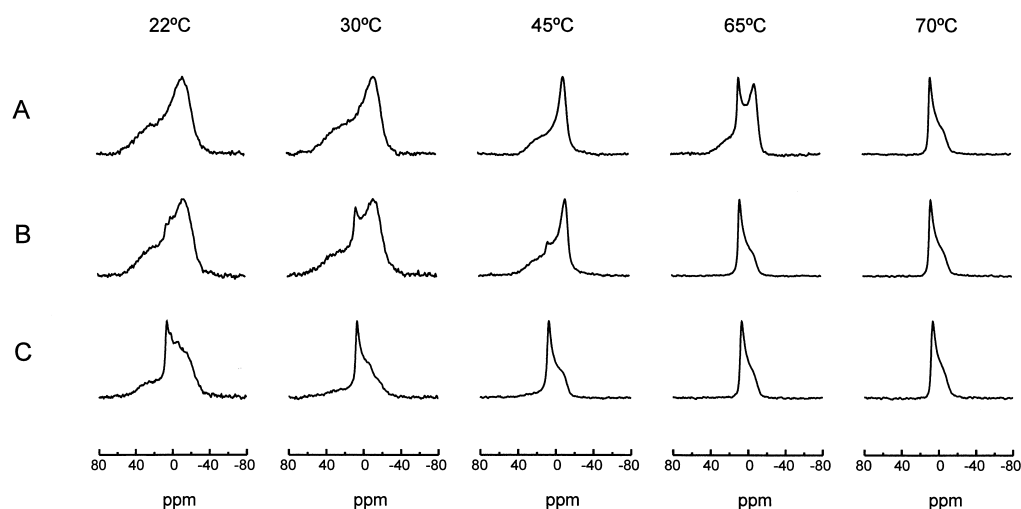


Fig. 4.  $^{31}\text{P}$ -NMR spectra of aqueous dispersions of mixtures of DEPE plus (+)-tatarol as a function of temperature. (A) Pure DEPE; (B) DEPE plus 2 mol% (+)-tatarol; (C) DEPE plus 10 mol% (+)-tatarol. Spectra have been normalized and temperatures are indicated on the spectra.

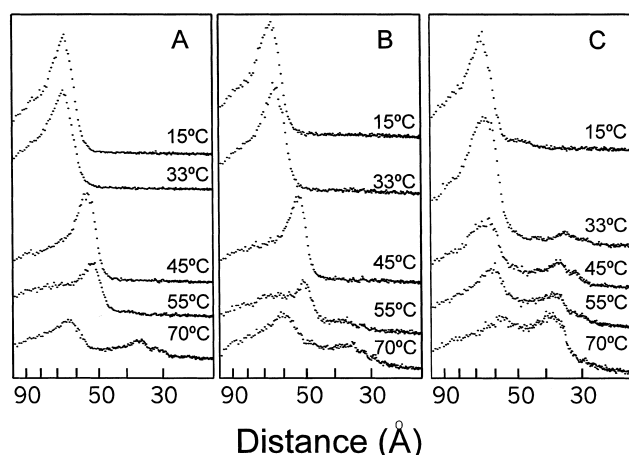


Fig. 5. X-Ray diffraction patterns for aqueous dispersions of DEPE and DEPE plus (+)-tatarol at the temperatures shown. (A) Pure DEPE; (B) DEPE plus 2 mol% (+)-tatarol; (C) DEPE plus 10 mol% (+)-tatarol. d-Spacings (Å) are plotted on a logarithmic scale.

lar state [26]. The results shown in Fig. 5 for pure DEPE model membranes indicate that between 15°C and 55°C pure DEPE adopts a lamellar structure, but at 70°C adopts a hexagonal- $H_{II}$  structure with reflections appearing at a ratio of  $1 : 1/\sqrt{3}$  [26]. The incorporation of 2 mol % of (+)-tatarol induced the coexistence of both lamellar and  $H_{II}$  phases at 55°C

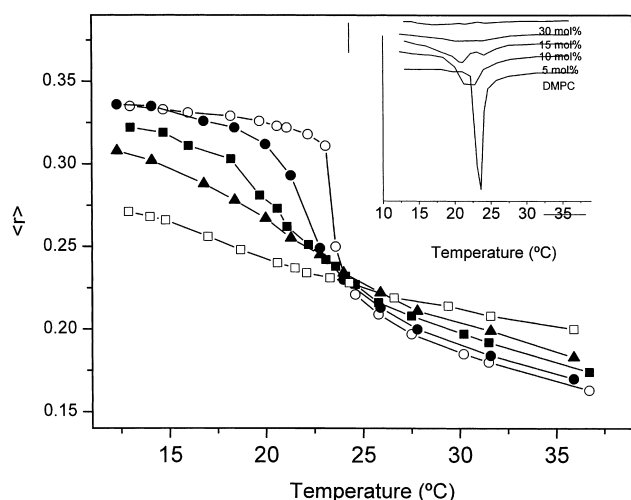


Fig. 6. Steady-state anisotropy,  $\langle r \rangle$ , of PA-DPH in aqueous dispersions of DMPC plus (+)-tatarol as a function of temperature for (○) pure DMPC and DMPC with (+)-tatarol at molar percentages of (+)-tatarol of (●) 5%, (■) 10%, (▲) 15% and (□) 30%. The insert shows the first derivative of the  $\langle r \rangle$  plots (see text for details).

(Fig. 5), whereas a concentration of 10 mol% of (+)-tatarol induced the coexistence of both lamellar and  $H_{II}$  phases at much lower temperatures, in accordance with the NMR results shown above (Fig. 4). There were also no significant differences in the d-spacings imposed by the presence of (+)-tatarol when compared with either pure DMPC or pure DEPE, indicating that the (+)-tatarol did not change the interbilayer repeat distance in either type of membrane.

The effect of (+)-tatarol on the structural order of lipid membranes was investigated by measuring as a function of temperature the steady-state fluorescence anisotropy,  $\langle r \rangle$ , of PA-DPH incorporated in DMPC vesicles and containing different mole fractions of (+)-tatarol. PA-DPH is a very useful molecule to study the structural order of the lipid bilayer since it anchors at the aqueous interface of phospholipid membranes by its carboxylate group whilst its fluorescent diphenylhexatrienyl moiety intercalates between the phospholipid acyl chains [27,28]. For pure DMPC,  $\langle r \rangle$  decreased slightly with increasing temperature, with a sharp drop occurring at 23°C, the  $T_c$  temperature (Fig. 6). Increasing gradually

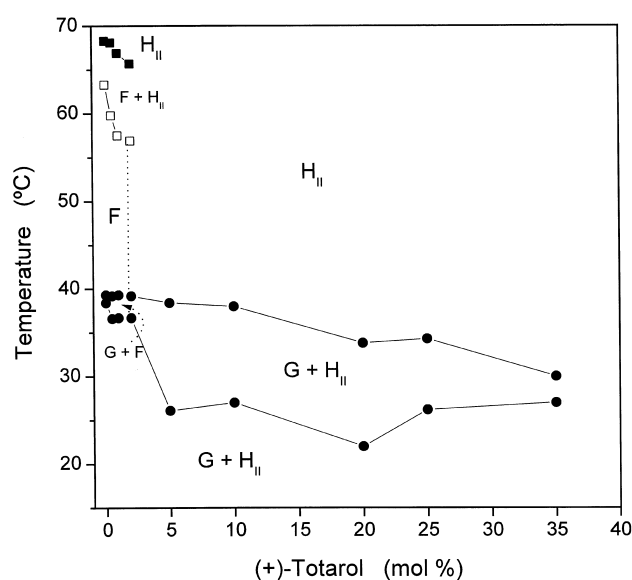


Fig. 7. Partial phase diagram for mixtures of DEPE plus (+)-tatarol. Open circles correspond to the lamellar solidus line and filled circles to the lamellar fluidus line. Open squares depict the fluid-lamellar/hexagonal- $H_{II}$  boundary and filled squares the fluid-lamellar+hexagonal- $H_{II}$ /hexagonal- $H_{II}$  boundary. G corresponds to a lamellar phase, F to a lamellar fluid phase and  $H_{II}$  to the hexagonal- $H_{II}$  phase (see text for details).

the mole fraction of (+)-tatarol up to 30 mol% it abolished the  $L_{\beta} \rightarrow L_{\alpha}$  phase transition and shifted it to lower temperatures (Fig. 6) in agreement with the DSC data. At temperatures below the main gel to liquid-crystalline phase transition it diminished the structural order of the phospholipid bilayer and at temperatures above it made the fluid phase more ordered. At 30 mol% of (+)-tatarol no transition was observed (Fig. 6). A similar effect has been reported for DMPC/cholesterol mixtures using different methods [29] and this supports the idea that (+)-tatarol intercalates between the phospholipid hydrocarbon chains [19]. The behaviour observed at a concentration of 10 mol% (+)-tatarol (see insert in Fig. 6) suggests the presence in the bilayer of different phospholipid domains, as previously indicated by the DSC experiments (Fig. 2A).

#### 4. Discussion

The diterpenoid (+)-tatarol is bacteriostatic towards a wide assortment of oral bacteria [13] and has a very high lipid/water partition coefficient  $K_p$  [19]. Although thymol, a bacteriostatic monoterpenoid, shares some structural features with (+)-tatarol, its lipid/water partition coefficient is much lower than that of (+)-tatarol [19]. The differences in lipid/water partition coefficients of both molecules imply that lower concentrations of exogenous (+)-tatarol would be required to achieve a 'critical' intramembranous concentration compared to thymol. Actually, we have found that lower concentrations of (+)-tatarol are necessary to show bacteriostatic activity against different oral bacteria than those of thymol (in preparation). Since (+)-tatarol is embedded in the phospholipid palisade of the membrane, with the phenol group located distant to the phospholipid/water interface [19], and is a larger molecule than thymol, (+)-tatarol may promote a greater degree of destabilization per molecule intercalated into the paraffinic core of the membrane [15,30,31].

DSC data indicate that (+)-tatarol disrupts the packing of the phospholipids, since it perturbed the cooperativity of the phase transitions of both DMPC and DMPG at concentrations as low as 2 mol%. This phenomenon could be explained in terms of intercalation of the diterpenoid between the phos-

pholipid molecules. A similar arrangement has been postulated for the diterpene resin acid abietic acid [22,32], which localizes its polar group (-COOH) in close proximity to the phospholipid ester moieties so that the molecule does not extend into the phospholipid bilayer beyond the C-4/C-7 carbons of the phospholipid molecule. At higher concentrations of (+)-tatarol, e.g. 10 mol%, several membrane components were observed, probably due to a lateral phase separation of (+)-tatarol rich domains. The decrease in  $T_c$  of membrane components was also accompanied by a decrease in  $\Delta H$ , indicating that (+)-tatarol perturbs the packing and interaction between the phospholipids. It has been described recently that different *n*-(9-anthroyloxy)stearic acid fluorescent probes could be incorporated efficiently into bacterial plasma membranes during the growth phase attaining high concentrations, i.e., between 7 and 13% [33]. As described above, lower concentrations of (+)-tatarol than these ones have significant effects on phospholipid membrane structure.

DSC,  $^{31}\text{P}$ -NMR, and small-angle X-ray diffraction were used to elucidate the molecular basis of the interactions between (+)-tatarol and DMPC, DMPG and DEPE membranes, to characterize the possible modulation by (+)-tatarol on the macroscopic organization of the phospholipids and construct the corresponding phase diagrams. The phase diagram for different DMPC/(+)-tatarol aqueous dispersions (not shown for brevity) showed that the temperature of the solidus line decreased with increasing concentration of (+)-tatarol, while the fluidus line slightly decreased up through 5 mol%. A temperature increase was subsequently observed on going from 5 to 15 mol% (+)-tatarol, indicating the likely presence of two different phospholipid domains in the fluid phase. In the region defined by the coexistence of the gel and fluid phases (G+F) at least two phospholipid domains coexist, since at least two peaks were observed. The behaviour of the solidus line in the partial phase diagram for DMPG plus (+)-tatarol (not shown) was similar to that described for DMPC plus (+)-tatarol, but the fluidus line decreased slightly up to 15 mol% (+)-tatarol. In both phase diagrams the phospholipid component evolved from a lamellar gel phase to a lamellar liquid-crystalline phase via a broad region of phase coexistence.



More complex phase behaviour was noted in mixtures containing DEPE plus (+)-tatarol, as shown by the corresponding phase diagram (Fig. 7). At concentrations of (+)-tatarol greater than 2 mol% the  $L_{\alpha} \rightarrow H_{II}$  phase transition peak was not observed due to broadening, though a shift to much lower temperatures could still be demonstrated by  $^{31}\text{P}$ -NMR spectroscopy and X-ray diffraction (Figs. 4 and 5). Up to 2 mol% (+)-tatarol the fluidus line corresponding to the  $L_{\beta} \rightarrow L_{\alpha}$  phase transition displayed immiscibility in the fluid state, indicating the presence of a DEPE/(+)-tatarol domain coexisting with free phospholipid. At about 2 mol% of tatarol, a complex pattern corresponding to domains with different DEPE/(+)-tatarol stoichiometries were observed. In the region defined by G+F there coexist two gel and fluid phases, but in the region defined by G+ $H_{II}$  at least three peaks were observed (Fig. 3). At high concentrations of (+)-tatarol, it appears that the  $L_{\alpha} \rightarrow H_{II}$  phase transition occurred at about the same temperature as the  $L_{\beta} \rightarrow L_{\alpha}$  phase transition. The  $^{31}\text{P}$ -NMR data support this interpretation and show that (+)-tatarol promotes formation of the hexagonal- $H_{II}$  phase at temperatures below the  $T_c$  of pure DEPE. The inclusion of (+)-tatarol in the DEPE membranes perturbs the lipid matrix and increases the acyl chain motion, which effectively increases the hydrophobic volume per molecule. Consequently, the formation of hexagonal structures would be facilitated by a large packing parameter [34]. Location of (+)-tatarol in the phospholipid bilayers should be compatible with its ability to perturb phospholipid model membranes. The fluorescence anisotropy data show that low concentrations of (+)-tatarol have strong effects on the anisotropy of PA-DPH, so that the diterpenoid is immersed in the phospholipid palisade and probably aligned along the phospholipid chains, with its phenol group located distant to the phospholipid/water interface [19].

Bacterial membranes contain significant amounts of lipids which can form inverted hexagonal- $H_{II}$  phases, such as diacylglycerols, phosphatidylethanolamines and phosphatidylglycerols [35,36]. The results of the present work, i.e., the complex thermotropic behaviour of phospholipid membranes containing (+)-tatarol indicative of the formation of perturbed membrane structures and the ability of (+)-tatarol in

promoting the hexagonal phase at low temperatures, indicate that the bactericidal and bacteriostatic actions of (+)-tatarol could be likely mediated through its interaction with the bacterial membrane. Work is in progress to elucidate the mechanism of its antibacterial activity in vivo.

### Acknowledgements

This work was supported by grant PM98-0100 from DGEIC, Madrid (to J.V.) and by funding from the Colgate Company, Piscataway, NJ (Zürich). We are grateful to Mr. Andreas Meier for expert technical assistance and to Prof. Dr. B. Guggenheim, Director of the Institut für orale Mikrobiologie und allgemeine Immunologie, for encouragement.

### References

- [1] S. Shapiro, A. Meier, B. Guggenheim, *Oral Microbiol. Immunol.* 9 (1994) 202–208.
- [2] M.E. Rodríguez-Linde, R.M. Díaz, A. García-Granados, J. Quevedo-Sarmiento, E. Moreno, M.R. Onorato, A. Parra, A. Ramos-Cormenzana, *Microbios* 77 (1994) 7–13.
- [3] J.E. Dellar, M.D. Cole, P.G. Waterman, *Phytochemistry* 41 (1996) 735–738.
- [4] L. Mendoza, M. Wilkens, A. Urzua, *J. Ethnopharmacol.* 58 (1997) 85–88.
- [5] T.L. Aceret, J.C. Coll, Y. Uchio, P.W. Sammarco, *Comp. Biochem. Physiol. C Pharmacol. Toxicol. Endocrinol.* 120 (1998) 121–126.
- [6] A. Urzua, M. Caroli, L. Vasquez, L. Mendoza, M. Wilkens, E. Tojo, *J. Ethnopharmacol.* 62 (1998) 251–254.
- [7] A. Ulubelen, G. Topcu, C. Eris, U. Sonmez, M. Kartal, S. Kurucu, C. Bozok-Johansson, *Phytochemistry* 36 (1994) 971–974.
- [8] O. Batista, A. Duarte, J. Nascimento, M.F. Simoes, M.C. de la Torre, B. Rodríguez, *J. Nat. Prod.* 57 (1994) 858–861.
- [9] M.O. Fatope, O.T. Audu, Y. Takeda, L. Zeng, G. Shi, H. Shimada, J.L. McLaughlin, *J. Nat. Prod.* 59 (1996) 301–303.
- [10] M. Hezari, R.E.B. Ketchum, D.M. Gibson, R. Croteau, *Arch. Biochem. Biophys.* 337 (1997) 185–190.
- [11] R. Benrezzouk, M.C. Terencio, M.L. Ferrándiz, A. San Feliciano, M. Gordaliza, J.M. Miguel del Corral, M.L. de la Puente, M.J. Alcaraz, *Life Sci.* 64 (1999) 205–211.
- [12] C. Zhang, M. Herari, M. Kuroyangi, B.K. Tan, *Pharmacol. Res.* 38 (1998) 413–417.
- [13] S. Shapiro, B. Guggenheim, *Quant. Struct.-Act. Relatsh.* 17 (1998) 327–337.

- [14] I. Kubo, H. Muroi, M. Himejima, *J. Nat. Prod.* 55 (1992) 1436–1440.
- [15] T. Mori, N. Matubayasi, I. Ueda, *Mol. Pharmacol.* 25 (1984) 123–130.
- [16] H. Haraguchi, H. Ishikawa, S. Sakai, B.P. Ying, I. Kubo, *Experientia* 52 (1996) 573–576.
- [17] K. Osawa, H. Yasuda, T. Maruyama, H. Morita, K. Takeya, H. Itokawa, K. Okuda, *Chem. Pharm. Bull.* 42 (1994) 922–925.
- [18] H. Haraguchi, S. Oike, H. Muroi, I. Kubo, *Planta Med.* 62 (1996) 122–125.
- [19] C.R. Mateo, M.J.E. Prieto, V. Micol, S. Shapiro, J. Villalain, *Biochim. Biophys. Acta* 1509 (2000) 167–175.
- [20] S. Shapiro, B. Guggenheim, *Oral Microbiol. Immunol.* 10 (1995) 241–246.
- [21] C.S.J. Böttcher, C.M. Van Gent, C. Priest, *Anal. Chim. Acta* 24 (1961) 203–204.
- [22] F.J. Aranda, J. Villalain, *Biochim. Biophys. Acta* 1327 (1997) 171–180.
- [23] J. Gallay, B. De Kruijff, *Eur. J. Biochem.* 142 (1984) 105–112.
- [24] T.D. Bradrick, E. Freire, S. Georgiou, *Biochim. Biophys. Acta* 982 (1989) 94–102.
- [25] J.A. Killian, F. Borle, B. De Kruijff, J. Seelig, *Biochim. Biophys. Acta* 854 (1986) 133–142.
- [26] V. Luzzati, H. Mustacchi, A. Skoulios, F. Husson, *Acta Crystallogr.* 13 (1962) 660–667.
- [27] P.J. Trotter, J. Storch, *Biochim. Biophys. Acta* 982 (1989) 131–139.
- [28] C.R. Mateo, M.P. Lillo, J. González-Rodríguez, A.U. Acuña, *Eur. Biophys. J.* 20 (1991) 41–52.
- [29] M. Bloom, E. Evans, O.G. Mouritsen, *Q. Rev. Biophys.* 24 (1991) 293–397.
- [30] L.M. Braswell, K.W. Miller, J.F. Sauter, *Br. J. Pharmacol.* 83 (1984) 305–311.
- [31] K. Tu, M. Tarek, M.L. Klein, D. Scharf, *Biophys. J.* 75 (1998) 2123–2134.
- [32] J. Villalain, *Biochim. Biophys. Acta* 1328 (1997) 281–289.
- [33] S. Natesan, C.N. Madhavarao, V. Sitaraman, *Biophys. Chem.* 85 (2000) 59–78.
- [34] J.N. Israelachvili, S. Marçelja, R.G. Horn, *Q. Rev. Biophys.* 13 (1980) 121–200.
- [35] C.R.H. Raetz, K.F. Newman, *J. Biol. Chem.* 253 (1978) 3882–3887.
- [36] R. Lill, W. Dowhan, W. Wickner, *Cell* 60 (1990) 271–280.